Received: 30 November 2022 | Revised: 19 January 2023 | Accepted: 20 January 2023

DOI: 10.1002/chir.23538

RESEARCH ARTICLE

Chirality WILEY

Impact of chiral ligands on photophysical and electro-optical properties of β-diketonate europium complexes in circularly polarized OLEDs

Francesco Zinna[1] | **Mariacecilia Pasini**[2] | **Matteo Cabras**[2] | **Guido Scavia**[2] | **Chiara Botta**[2] | **Lorenzo Di Bari**[1] | **Umberto Giovanella**[2]

[1]Dipartimento di Chimica e Chimica Industriale, Università di Pisa, Pisa, Italy

[2]Consiglio Nazionale delle Ricerche, Istituto di Scienze e Tecnologie Chimiche "Giulio Natta", Milan, Italy

Correspondence

Lorenzo Di Bari, Dipartimento di Chimica e Chimica Industriale, Università di Pisa, via Moruzzi 13, 56124. Pisa, Italy.
Email: lorenzo.dibari@unipi.it

Umberto Giovanella, Consiglio Nazionale delle Ricerche, Istituto di Scienze e Tecnologie Chimiche "Giulio Natta" via A. Corti 12, 20133. Milan, Italy.
Email: umberto.giovanella@scitec.cnr.it

Funding information

Italian University and Research Ministry, Grant/Award Number: PRIN Project 20172M3K5N; University of Pisa, Grant/Award Numbers: PRA 2020_21, 2019_23

Abstract

Luminescent lanthanide complexes exhibiting chiroptical properties are attracting attention for their application in chiral optoelectronics and photonics, thanks to their unique optical properties, allied to intraconfigurational f–f transitions, which are generally electric-dipole-forbidden and can be magnetic dipole-allowed, which in an appropriate environment can lead to high dissymmetry factors and strong luminescence, in the presence of an antenna ligand. However, because luminescence and chiroptical activity are governed by different selection rules, their successful application in commonly used technologies is still an expectation. Recently, we showed that europium complexes bearing β-diketonates acting as luminescence sensitizers, and chiral bis(oxazolinyl) pyridine derivatives as the chirality inducer, reasonably perform in circularly polarized (CP) organic light-emitting devices (OLEDs). Indeed, europium β-diketonate complexes are an interesting molecular starting point, given their strong luminescence and their established use in conventional (i.e., nonpolarized) OLEDs. In this context, it is interesting to investigate in detail the impact of the ancillary chiral ligand on complex emission properties and the performances of corresponding CP-OLEDs. Here we show that, by incorporating the chiral compound as emitter in the architecture of solution processed electroluminescent devices, CP emission is retained, and the efficiency of the device is comparable to reference unpolarized OLED. The observed remarkable dissymmetry values strengthen the position of chiral lanthanide-OLEDs as CP-emitting devices.

KEYWORDS

chiral emission, circularly polarized emission, electroluminescence, europium complex, lanthanides, OLED

[This article is part of the Special issue: Chiral Materials. See the first articles for this special issue previously published in Volumes 34:12, 35:2, 35:3 and 35:4. More special articles will be found in this issue as well as in those to come.]

1 | INTRODUCTION

The development of chiral lanthanide (Ln) complexes featuring at the same time a decent photoluminescence (PL) quantum yield (PLQY) and a good circularly polarized PL (CPPL) efficiency has presented a continuous challenge. CPPL efficiency is quantified by the dissymmetry factor (g_{PL}) defined as $2(I_L - I_R)/(I_L + I_R)$, where I_L and I_R refer to the intensity of left and right circularly polarized (CP) light, respectively.[1] g_{PL} is not correlated to PLQY because total emission and CPPL are governed by different selection rules. A convenient metrics, which takes into account both parameters, is the CPPL brightness (B_{CPPL}), defined as[2] $B_{CPPL} = \varepsilon \cdot PLQY \cdot |g_{PL}|/2$, where ε is the molar extinction coefficient at the excitation wavelength. A maximized B_{CPPL} is one of the desired features of a good molecular candidate for efficient CP-OLEDs.

The first requirement when designing efficient luminescent Ln(III) complexes is a suitable antenna ligand, that is, a moiety able to sensitize the emission of f–f transitions.[3] Accordingly, the PL process of Ln(III) complex takes place by means of energy transfer (ET), usually from the triplet level of ligand to the ion center. Besides that, other mechanisms may be at play, such as ET from the singlet state, internal ligand charge transfer (ILCT) state, and ligand-to-metal charge transfer (LMCT).[4–6] More specifically, strong Ln(III)-based emitters require ligands, which ensure high UV-light absorption, efficient ET to the central Ln(III) ion, a stable coordination geometry, and exclusion of solvent molecules from the first sphere, to avoid nonradiative decays. All these functions can be realized by one type of ligand in homoleptic complexes or two different ones in heteroleptic complexes.[7]

Among efficient Eu(III)-based emitters, β-diketonate Eu(III) complexes are superior to other complexes as demonstrated by their large employment for the fabrication of organic light-emitting devices (OLEDs)[5,8,9] with external quantum efficiencies (EQEs) and luminance exceeding 7% and 2000 cd/m^2, respectively.

The 2-thenoyltrifluoroacetonate (TTA) is one of the most widely used β-diketonates anionic ligands for efficient sensitization of Eu ions. Its combination with 1,10-phenanthroline (Phen), or its derivatives, boosts the PLQY of heteroleptic Eu(III) complex (commonly known as Eu(TTA)$_3$Phen, Scheme 1B) above 70% in solid state. The efficiency and luminance of corresponding OLEDs has settled to the values of ∼1.3% and 137–505 cd/m^2,[10–12] if fabricated from vapor-phase, and ∼10^{-2}% and 417 cd/m^2 for solution processed ones.[9,13] Interestingly, besides its application in OLED technology, the Eu(TTA)$_3$Phen has been lately proposed for a wide range of applications[14,15] like ultraviolet detection,[16,17] luminescent solar concentrators,[18] lasers[19] and temperature sensors.[20,21]

A viable strategy to achieve CPL signals in Eu(III) complexes (but valid also for Ln complexes in general) has been the introduction of dissymmetry elements to well-developed chromophoric ligand systems.[22–24]

Following this approach, chiral β-diketonate Eu(III) complexes, featuring high g_{PL}, have been proposed with B_{CPPL} around 50–100 M^{-1} cm^{-1}.[2] Yuasa and coworkers[25] prepared chiral Eu complexes based on Eu(HFA)$_3$ (HFA: 1,1,1,5,5,5-hexafluoropentane-2,4-dione), where the coordination sphere is completed by chiral bis(oxazolinyl) pyridine (pybox) auxiliary ligands, with different terminal substituents. Specifically,

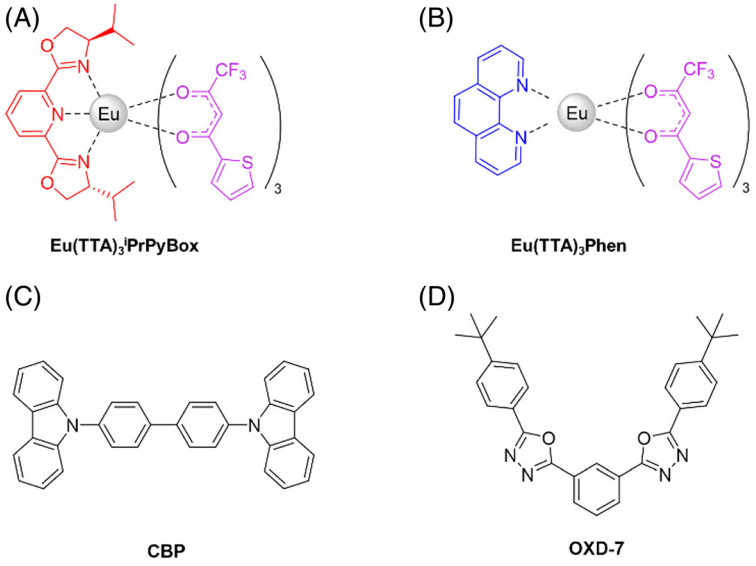

SCHEME 1 Chemical structure of (A) Eu(TTA)$_3$(*R,R*)-^{i}PrPyBox, hereafter Eu(TTA)$_3$^{i}PrPyBox, and (B) Eu(TTA)$_3$Phen complexes, (C) 4,4′-Bis(*N*-carbazolyl)-1,1′-biphenyl (CBP) and (D) 1,3-bis[2-(4-tert-butylphenyl)-1,3,4-oxadiazo-5-yl] benzene (OXD-7)

Eu(HFA)$_3$(*R*)-(iPrPyBox) shows a very large | g_{PL} | value (0.46) as well as high PLQY (41%) in acetonitrile. Alternatively, the use of TTA instead of HFA leads to | g_{PL} | values of 0.24 in CH_2Cl_2[24] and 0.75 in toluene.[26]

The expectation to benefit from such a strong CP emission also from electrically generated excitons by fabricating CP-OLEDs[27] raises the bar to a next level of challenge. Notable examples of chiral Eu(III) complexes used as emitter in CP-OLEDs were recently reported by our groups.[1,26,28] Devices based on CsEu(hfbc)$_4$ (hfbc = heptafluorobutyrylcamphorate) showed remarkable g_{EL} values up to 1 but with efficiencies lagging at least one order of magnitude behind values of conventional (unpolarized) Eu-based OLEDs.[5] Successively, the use of Eu(TTA)$_3$(*R*)-iPrPyBox (iPrPyBox = 2,6-Bis[4-isopropyl-2-oxazolin-2-yl]pyridine) has enhanced CP-OLEDs performance, maintaining a good | g_{EL} | value (0.51 at 592 nm).[26]

Despite the accumulated knowledge on complexes of Eu(III) with β-diketonate type of ligands, like Eu(TTA)$_3$Phen, there is still room for improvement in the fundamental understanding of the properties of these compounds, when they are provided with CP emission.

For that reason, in the following, we evaluate the impact of the chiral ligand on the photophysical and electro-optical properties of enantiopure Eu(TTA)$_3$iPrPyBox, analyzed with respect to the reference Eu(TTA)$_3$Phen complex.

2 | MATERIALS AND METHODS

2.1 | Materials

The chiral Eu(III) complex Eu(TTA)$_3$(*R,R*)-iPrPyBox features TTA and 2,6-Bis(4-isopropyl-2-oxazolin-2-yl)pyridine (iPrPyBox), whereas the achiral complex Eu(TTA)$_3$Phen features TTA and 1,10-phenanthroline as ancillary ligand (Scheme 1). Complexes were synthesized as reported earlier.[24,25,29] Here, only the properties of the Eu(TTA)$_3$(*R,R*)-iPrPyBox enantiomer is discussed.

2.2 | Characterization

Electronic absorption spectra were carried out on a Perkin-Elmer Lambda 900 UV–VIS–NIR Spectrometer. ECD spectra were recorded with a Jasco J-1500 spectropolarimeter. Steady-state and time-resolved PL spectra were recorded on a modified Jobin-Yvon Horiba Fluorolog spectrofluorimeter. PLQYs have been obtained for solutions by using quinine sulfate as a reference and in the solid state with a homemade integrating sphere, as reported elsewhere.[30] CPPL and CPEL activities are evaluated by means of a fixed linear polarizer (LP) and a rotating quarter wave plate (QWP) placed in front of the CCD detector, as previously described.[1]

2.3 | Devices

For the manufacturing of the devices indium tin oxide (ITO) was used as anode. After sequential cleaning of the ITO-coated glass of 2.5 cm × 2.5 cm in acetone and isopropanol in a sonicator for 10 min in each solvent at 50°C, it was treated with a nitrogen plasma. PEDOT:PSS Clevios VPI 4083 was spin-coated to a 35-nm thickness. PVK (35 nm) film is deposited on top of PEDOT:PSS from a 10-mg/mL chlorobenzene solution. Solutions of the different emitters with the selected host matrix (CBP and OXD-7) in $CHCl_3$ or toluene at a total concentration of 15 mg/mL were spin-coated on top of the glass/ITO/PEDOT:PSS/PVK substrate. The TPBI electron transport/hole-blocking layer (30 nm) was deposited using an organic molecular beam deposition (OMBD) system. Finally, 1.5 nm of LiF and 6 to110 nm of Al were thermosublimated inside the high vacuum evaporator to achieve a transparent or mirror cathode. Photons emitted in forward direction through the glass substrate were collected by a calibrated photodiode. Current density-luminance-voltage curves were recorded by Keithley 2602 apparatus. Luminance of the OLEDs was directly measured by means of Konica-Minolta LS-150 luminance meter.

3 | RESULTS AND DISCUSSION

3.1 | Photophysical characterization

The impact of the chiral ligand on the photophysical properties of Eu(TTA)$_3$iPrPyBox with respect to Eu(TTA)$_3$Phen (Scheme 1) is evaluated by means of absorption and PL studies, both steady-state and time-resolved, PLQY, on solutions and thin films.

Absorption spectra of both solutions show a main band at about 350 nm assigned to TTA, and a second band around 270 nm associated to both TTA and Phen or iPrPyBox.

PL spectra feature characteristic $^5D_0 \rightarrow {}^7F_j$ (j = 0–4) Eu-centered transitions.[22] Complexes are excited at 350 nm, where absorption of both Phen and iPrPyBox is negligible, and the sensitization of the Eu ion mainly occurs through TTA excitation. In particular, we may focus on the most intense electric-dipole transitions $^5D_0 \rightarrow {}^7F_2$ around 615 nm (also called hypersensitive transition) and on the highly CP magnetic-dipole

transitions $^5D_0 \rightarrow {}^7F_1$ around 590 nm (Figure 2A,B). Different shape and full width-at-half-maximum (FWHM), mainly for the hypersensitive transition, are observed for the two complexes, due to a different crystal field and overall geometry caused by either Phen or ^{i}PrPyBox. We recall that Phen and ^{i}PrPyBox are bi- and tridentate ligands, respectively. The relative integrated intensity of the $^5D_0 \rightarrow {}^7F_2$ transition with respect to that of the $^5D_0 \rightarrow {}^7F_1$ (hereafter indicated as A_{21}) in the Eu(III) complex measures the symmetry of the coordination sphere,[31] and the distortion of the symmetry around the Eu(III) ion enhances the probability of the electric-dipole transition. A_{21} values of 16.30 and 15.63, calculated for Eu(TTA)$_3$^{i}PrPyBox and Eu(TTA)$_3$Phen, respectively (Table S1), are considerably large[32] indicating a reduction of the symmetry around Eu ions with respect to other β-diketonate Eu(III) complexes.[29]

CPPL activity is evaluated by means of a fixed LP and a rotating QWP. The introduction of the chiral ^{i}PrPyBox ligand imparts the desired circular polarization of the emitted light with respect to reference Eu(TTA)$_3$Phen complex. Indeed, Eu(TTA)$_3$^{i}PrPyBox shows a strong chiroptical activity with g_{PL} of −0.76 at 592 nm accompanied by values of −0.25 at 585 nm and 0.06 at 612 nm in toluene.

Despite a lower PLQY (0.30) observed with respect to Eu(TTA)$_3$Phen (0.48), the Eu(TTA)$_3$^{i}PrPyBox complex exhibits excellent value of B_{CPPL} 103.7 m^{-1} cm^{-1} at 592 nm (Table 1) with respect to other chiral Eu(III) complexes.[2,24]

Typically, the PLQY of Eu(III) complex can be related to the efficiency of the ligand-Eu ET and the ligand intersystem crossing. It is given by $PLQY = \eta_{sens} PLQY^{Eu}{}_{Eu}$, where intrinsic $PLQY^{Eu}{}_{Eu}$ results from direct Eu excitation, and η_{sens} represents the efficiency of the overall sensitization process, from the surroundings onto the metal ion (i.e., sensitization efficiency). $PLQY^{Eu}{}_{Eu}$ can be expressed (details of the calculations are reported in ref.[29]) as the ratio between observed lifetime (τ_{obs}) and radiative lifetime (τ_{rad}). The values of τ_{obs} for both Eu(III) complexes (574 and 710 μsec for Eu(TTA)$_3$^{i}PrPyBox and

TABLE 1 Summary of photophysical properties of Eu(TTA)$_3$^{i}PrPyBox and Eu(TTA)$_3$Phen in toluene solution and as thin films

	Solution			
Compound	**PLQY**	**τ_{obs}, (μsec)**	**g_{PL}, [nm]**	**B_{CPPL} (m^{-1} cm^{-1})[nm]**
Eu(TTA)$_3$^{i}PrPyBox	0.30	574	−0.25 [585] −0.75 [592] 0.06 [612]	103.7 [592] 84.2 [615]
Eu(TTA)$_3$Phen	0.48	710	none	/

[a]10 wt.% Eu-doped PMMA.
[b]6 wt.% Eu-doped CBP:ODX-7.
[c]Excitation at 350 nm.
[d]Excitation at 380 nm.
[e]Type-A devices.
[f]Type-B devices.

TABLE 1 (Continued)

	Film						Devices	
	PMMA[a]			CBP:OXD-7[b]				
Compound	**PLQY**	**<τ_{obs}>, μsec[b]**	**g_{PL}, [nm]**	**PLQY**	**<τ_{obs}>, (μsec)**	**g_{PL}, [nm]**	**EQE_{MAX} (%)**	**g_{EL}, [nm]**
Eu(TTA)$_3$^{i}PrPyBox	0.55	689	−0.21 [585] −0.59 [592] 0.03 [612]	0.53	710[c] 610[d]	−0.53 [593]	1.01[e] 0.34[f]	−0.63[f] [592]
Eu(TTA)$_3$Phen	0.68	712	none	0.73	676[c] 642[d]	/	1.18[e] 0.76[f]	/

[a]10 wt.% Eu-doped PMMA.
[b]6 wt.% Eu-doped CBP:ODX-7.
[c]Excitation at 350 nm.
[d]Excitation at 380 nm.
[e]Type-A devices.
[f]Type-B devices.

$Eu(TTA)_3Phen$, respectively) are obtained by single-exponential fits of the PL decays in solution indicating the presence of only one emissive Eu(III) center. From τ_{obs}/τ_{rad} ratios, we estimated $PLQY^{Eu}_{Eu}$ of ~50% for both complexes. The η_{sens} calculated from the ratio $PLQY/PLQY^{Eu}_{Eu}$ are nearly complete (~96%) for $Eu(TTA)_3Phen$ and become smaller for $Eu(TTA)_3{}^{i}PrPyBox$ (~60%) (Table S1). Additionally, the nonradiative deactivation rate (A_{NR}) of $Eu(TTA)_3{}^{i}PrPyBox$ is slightly higher than the one calculated for $Eu(TTA)_3Phen$, with a reduction in excited state lifetime (Table S1). The presence of more efficient quenching pathways for $Eu(TTA)_3{}^{i}PrPyBox$ could be related to an increased vibrational quenching due the presence of additional aliphatic CH_3 groups in the vicinity of the Eu center and not present in $Eu(TTA)_3Phen$.[33] Both Phen and $^{i}PrPyBox$ ligands are effective in avoiding the coordination of water at the metal center, which would further decrease the PLQY.[24,29]

The PLQY can vary with solvent polarity because the ligand fields of C_3-symmetric complexes are extremely sensitive to such parameter, even when solvent is not present in the first coordination sphere.[24,34] In solid state, also the rigidity of the environment could impact on the symmetry of a Eu complex,[29] hence on its photophysical properties. Understanding this behavior is crucial for the fabrication of device prototypes. Indeed, the common strategy to manufacture solution processed Eu-based OLEDs involves, not a neat Eu-complex based active layer but a dispersion of the complex in a host matrix[6] that provides a proper environment for the efficient emission of the Eu sites, (i.e., dispersion of Eu-complex, bipolar charge transport, and exciton confinement at Eu sites).

The easiest way to get preliminary information about the photophysics of complexes in a solid-state dispersion is their blending with inert transparent polymer matrix, such as poly (methyl methacrylate) (PMMA). The absorption and PL spectra (excited at 350 nm) of PMMA:Eu complexes films (Figure 1C,D) are similar to corresponding solutions (Figure 1A,B) but are very different in their PLQYs and g_{PL} values. An increase in PLQY of both complexes in PMMA with respect to solutions (~40% increase for $Eu(TTA)_3Phen$ and of over 80% for $Eu(TTA)_3{}^{i}PrPyBox$) is observed as well as of the average τ_{obs} values ($<\tau_{obs}>$), obtained from bi-exponential fits for the solid samples. The bi-exponential behavior is probably due to different conformational arrangements of the ligands around the Eu center, stabilized by the PMMA matrix. The distortion of the symmetry around the Eu(III) ion in solid state enhances the probability of the electric-dipole transition[29] but, at the same time, slightly reduces the chiro-optical activity ($g_{PL} = -0.59$ at 592 nm) compared to toluene solution.

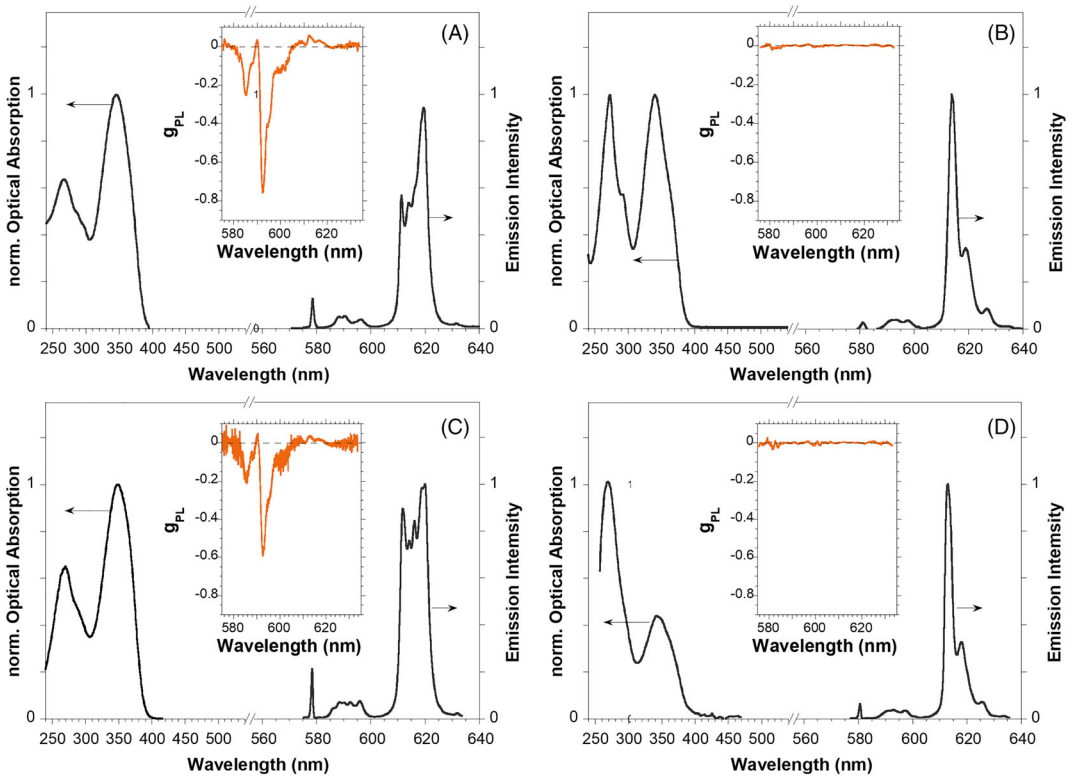

FIGURE 1 Absorption, PL spectra (excitation 350 nm) and dissymmetry factor g_{PL} (insets) for toluene solution (top) and PMMA film (bottom) loaded with $Eu(TTA)_3{}^{i}PrPyBox$ (A,C) and $Eu(TTA)_3Phen$ complexes (B,D).

The dispersion of the complexes in a matrix with bipolar charge transport characteristics and highest occupied/lowest unoccupied molecular orbital (HOMO/LUMO) energy levels suitable for proper charge injection is a critical demand in the purpose of fabricating efficient electroluminescent devices. In addition to a balanced charge carrier transport/injection, strong PLQYs are pursued through the spectral overlapping between PL of the matrix and absorption of the complexes (Figure S1). This is done to favor a resonant energy transfer (FRET) from the energy donor host matrix to the TTA ligands of the Eu-complex acceptor. In fact, the FRET mechanism promotes the radiative recombination at the complex, hence positively impacting on device performance.

In this view, the combination of the small molecule 4,4-N,N′-dicarbazolyl-1,1′-biphenyl (CBP) as hole transporter and the electron transporting 1,3-bis[2-(4-tert-butylphenyl)-1,3,4-oxadiazo-5-yl]benzene (OXD-7), in the ratio 1:1 by mass, is proposed[35] for the role of the host. The two Eu complexes are dispersed in CBP:OXD-7 in the equal molar concentration.

HOMO/LUMO energy levels[26,29] of Eu(TTA)$_3$^{i}PrPyBox and Eu(TTA)$_3$Phen are −2.56/−5.7 eV and −3.05/−5.9 eV, respectively, and well match with HOMO/LUMO of CBP:OXD-7 host.

Absorption and excitation (PLE) spectra of both Eu(III)-based blend films resemble the absorption spectrum of the undoped CBP:OXD-7 (Figure 2A), hence demonstrating the occurrence of the FRET in both blends. Notably, the OXD-7 plays an important

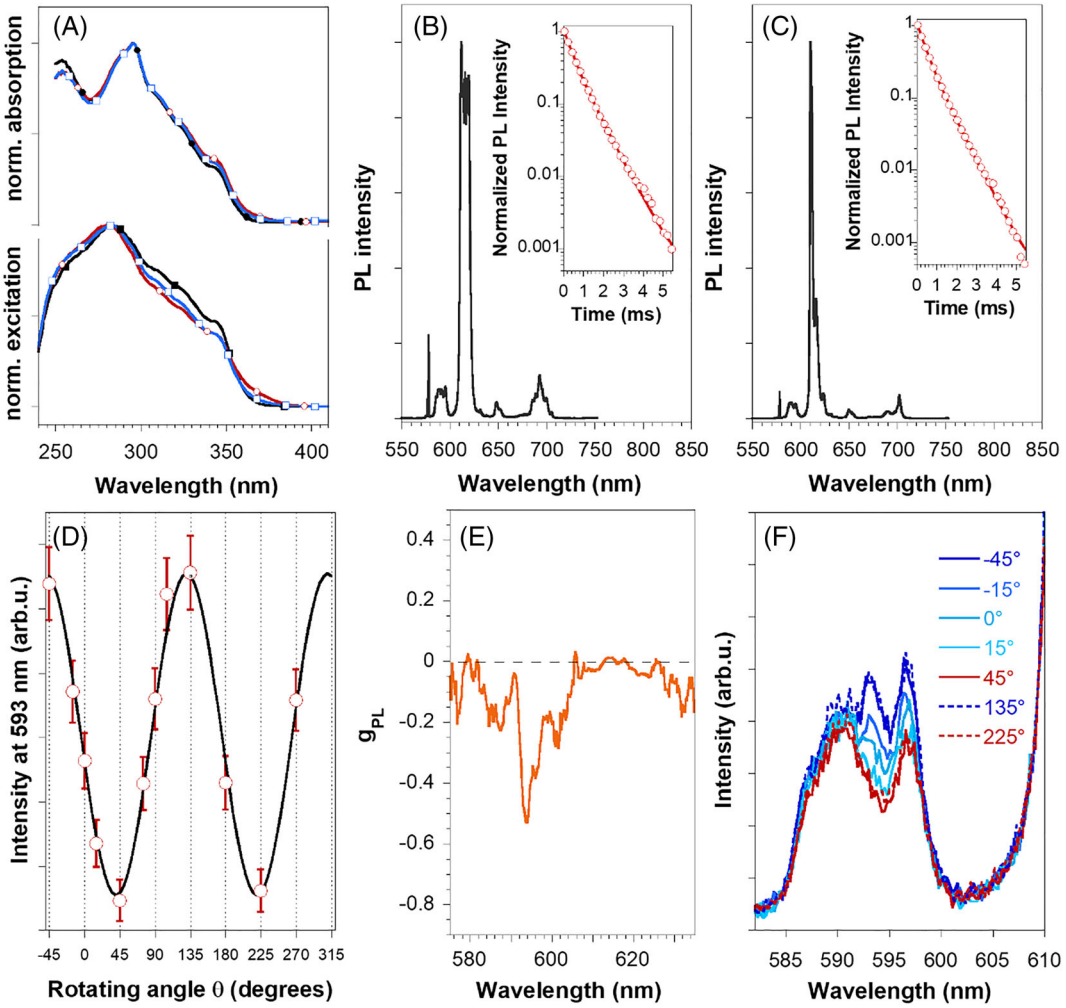

FIGURE 2 (A) Normalized absorption and PLE spectra of CBP:OXD-7 film (black ■), monitored at 450 nm, and of blends with Eu(TTA)$_3$^{i}PrPyBox (blue □) and Eu(TTA)$_3$Phen (red ○), monitored at 611 nm; PL spectra (exc. 350 nm) of CBP:OXD-7 blends of Eu(TTA)$_3$^{i}PrPyBox (B) and Eu(TTA)$_3$Phen (C); in the insets, corresponding PL decays (excitation at 380 nm; emission 615 nm (B) and 610 nm (C) with bi-exponential fits); (D) oscillation of emission intensity as a function of the angle θ for CBP:OXD-7:Eu(TTA)$_3$^{i}PrPyBox film; (E) g_{PL} of CBP:OXD-7:Eu(TTA)$_3$^{i}PrPyBox film and (F) emission intensity for the $^5D_0 \rightarrow {}^7F_1$ transition with respect to θ.

role in FRET mechanism because excited CBP singlet energies are only partially transferred to $Eu(TTA)_3Phen$ singlet states.[12] Similarity between PLQY values and decay times of both complexes in their PMMA and CBP:OXD-7 blends (inset of S2, Figure 2B,C and Table 1) excludes the back-transfer[29] as a relief quenching mechanism.

Both PL spectra (Figure 2B,C) and chiroptical properties are not significantly affected by switching from PMMA to CBD:OXD-7 matrix. The emission intensity of both $Eu(TTA)_3{}^{i}PrPyBox$ blends films (Figure S3 and Figure 2D) periodically decreases and increases as a function of the angle θ of the easy axis of the rotating QWP with respect to the axis of the fixed LP. The oscillation pattern, with a periodicity of 180°, indicates that no appreciable linearly polarized components are present, and it is well reproduced by the fitting curve provided by Eq. $I = I_L \cos^2(\theta + \pi/4) + I_R \sin^2(\theta + \pi/4)$, with θ in radians.[36] The minimal or maximal values appear at $\theta = 45$, 135, 225, and 315°, corresponding to the right- and left-CPL intensity that leads to $g_{lum} = -0.55$ and -0.53 at 593 nm (Figure 2E) for PMMA and CBP:OXD-7 blends, respectively, in agreement with previous data.[26] Figure 2F shows the total emission intensity for $^5D_0 \rightarrow {}^7F_1$ transition as a function of θ for CBP:OXD-7:$Eu(TTA)_3{}^{i}PrPyBox$ film.

4 | ELECTROLUMINESCENT DEVICES

Eu-doped CBP:OXD-7 films are incorporated as active layer in the multilayer architecture of solution processed electroluminescent devices. The designing of OLEDs with multiple layers is a way to reduce the energy barrier for charge transport through the device. For this reason, a polyvinylcarbazole (PVK) is used to bridge the energy barrier for hole injection while also playing an electron blocking role.[37] On the other hand, the electron transporting/injecting 2,2′,2″-(1,3,5-benzinetriyl)-tris(1-phenyl-1-H-benzimidazole) (TPBI) facilitates the electron injection from the cathode, and it is also involved with hole-blocking and exciton confinement.

The thickness of the organic semiconductor layers, both active and charge regulating layers, affects the location of the recombination zone of radiative excitons within the active layer and hence impacts on the device EQE and CP activity.[28] The transparency of the cathode is an even more critical issue because the reflection on the cathode causes a reversal of handedness of the incident CP light; hence, decreasing the polarization of photons collected at the exit of the device. On the other hand, if the photons pass though the cathode, instead of being reflected, the

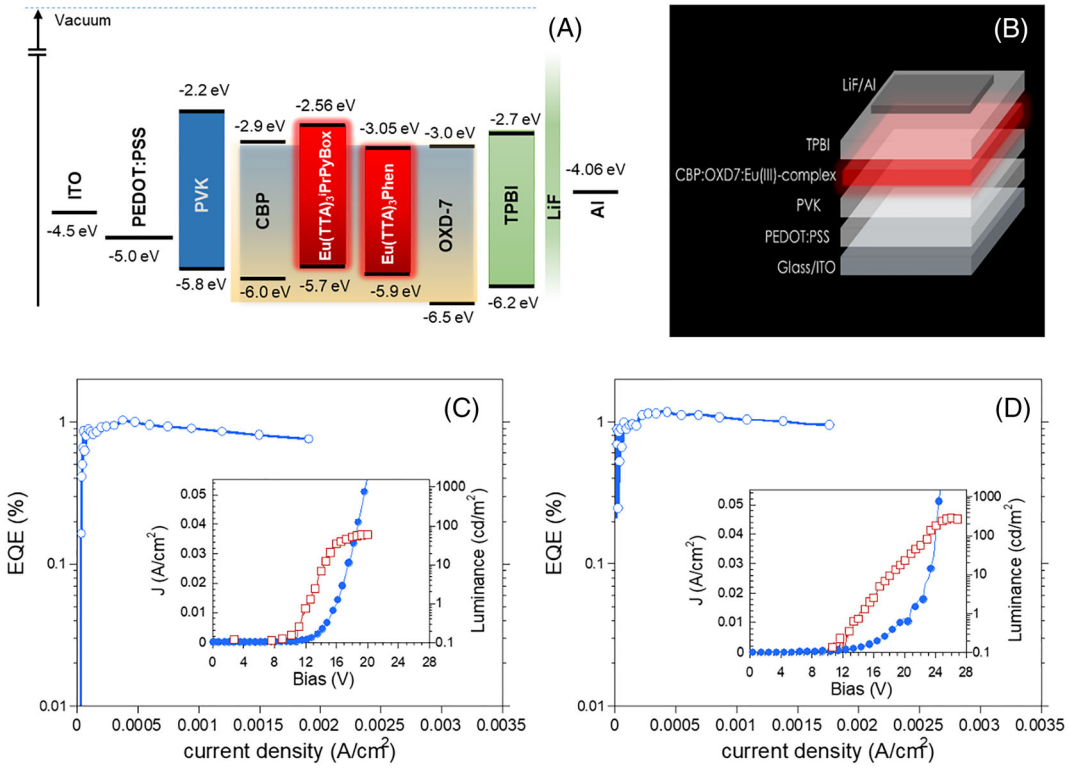

FIGURE 3 Flat-band energy-level diagram (A); image of device architecture (B), EQE vs. J for representative Type-A device embedding $Eu(TTA)_3{}^{i}PrPyBox$ (C) and $Eu(TTA)_3Phen$ complexes (D); inset, JLV characteristic curves, showing maximum luminance of representative Type-A devices

EQE measured at the surface of the transparent substrate is lowered because less photons are collected.[1]

Consequently, to target at the same time high efficiency of the device and large dissymmetry factor, CP-OLEDs with active and functional layer with a defined thickness,[28] and partially transparent cathode, are designed.

The semiconducting layers are processed by spin-coating to form films with thickness of 35 nm for PVK, 80 nm for the active layer. The active layer is covered by a thin (30 nm) vacuum-growth layer of TPBI. HOMO/LUMO levels of all components of the device architecture are reported in a flat-band energy-level diagram (Figure 3A).

Devices with two configurations, that is, total reflective (Type-A devices) and maximal transparency (Type-B devices), are manufactured with the architecture ITO/PEDOT:PSS/PVK/CBP:OXD-7:Eu-complex/TPBI/LiF/Al (Figure 3B).

Films of the two blends deposited over a PVK-covered substrate show similar topography with surface root-mean-square roughness in the range of 0.21–0.24 nm (Figure S4).

The electroluminescence (EL) spectra of both $Eu(TTA)_3{}^{i}PrPyBox$ and $Eu(TTA)_3Phen$ devices (Figure 4C,D) show typical Eu-centered transitions. A neat CPEL is observed in $Eu(TTA)_3{}^{i}PrPyBox$-based OLEDs, which, as expected, is dependent on the reflectivity of the cathode.

A remarkable EL dissymmetry factor (g_{EL}) of −0.63 (inset of Figure 4C) is observed in Type-B configuration for the $^5D_0 \rightarrow {}^7F_1$ transition at 592 nm. Such a g_{EL}, that is among the highest value observed lately,[1,28,38–40] indicates that a high degree of electrically generated CPEL at 592 nm (with a ratio about 66/34 of right/left polarized photons) can be achieved once the reflection on the back electrode is appropriately adjusted.

CBP hole transporting host has advantages[35] over PVK used in active layers of earlier devices.[26] CBP displays higher hole mobility ($2{\cdot}10^{-3}$ $cm^2V^{-1}s^{-1}$)[41] with respect to PVK ($4.8{\cdot}10^{-9}$ $cm^2V^{-1}s^{-1}$).[42] Moreover, CBP:OXD-7:$Eu(TTA)_3{}^{i}PrPyBox$ film shows higher PLQY and longer lifetimes (0.53 and 710 μs) than PVK:OXD-7:$Eu(TTA)_3{}^{i}PrPyBox$ one (∼0.25 and 565 μs[26]). The similar PL decay times in PMMA and CBP:OXD-7 matrix further suggest that CBP:OXD-7 is a better suited host for the Eu(III) complex than PVK[26]

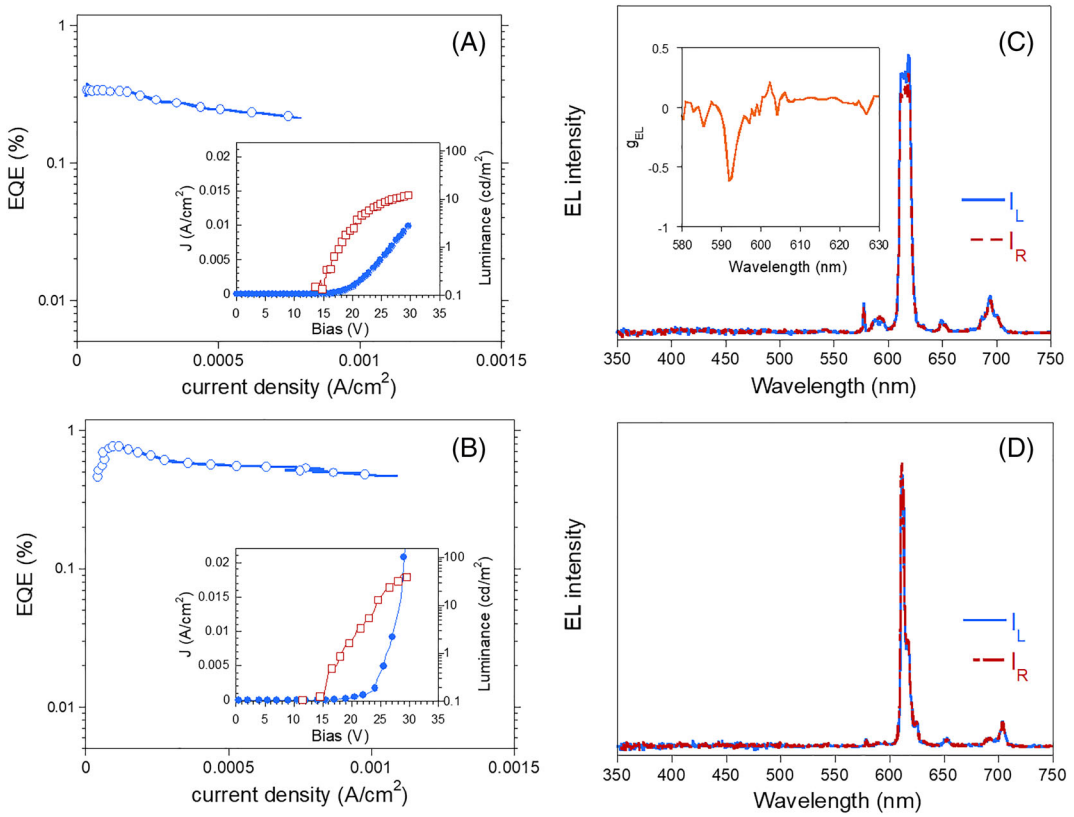

FIGURE 4 EQE vs J for representative Type-B devices embedding $Eu(TTA)_3{}^{i}PrPyBox$ (A) and $Eu(TTA)_3Phen$ complexes (B); inset, JLV showing maximum luminance of representative devices; EL spectra (dashed red and solid blue lines for the two CP components) of devices embedding $Eu(TTA)_3{}^{i}PrPyBox$ (C) and $Eu(TTA)_3Phen$ complexes (D); inset of (C) g_{EL} for CP-OLED

also resulting in slightly amplified g_{EL} value with respect to corresponding g_{PL}.

Total reflective Eu(TTA)$_3$^{i}PrPyBox-based CP-OLED exhibited a maximum EQE of 1.01% at 0.4 mA/cm^2 measured in forward configuration. This quite notable EQE value, very close to 1.18% recorded for Eu(TTA)$_3$Phen-based OLEDs (Figure 3C,D), is comparable to Eu-based OLEDs data reported in literature,[9,43] and this is two times higher than recent published performance in the framework of CP-OLEDs.[26] The maximum luminescence recorded for Type-A Eu(TTA)$_3$^{i}PrPyBox-based CP-OLEDs (60 cd/m^2) is 4–5 times lower than for Eu(TTA)$_3$Phen-based devices (287 cd/m^2). Recently, the lifetime of the complex has been proposed as an hampering factor for high luminescence,[9] but the variation in recorded $<\tau_{obs}>$ for the two CBP:OXD-7 blends cannot explain the variation in OLED luminance. Most probably, one of the causes should be find in the lower PLQY of Eu(TTA)$_3$^{i}PrPyBox with respect to Eu(TTA)$_3$Phen, in both solution, PMMA and CBP:OXD-7 blends. The position of the LUMO level of Eu(TTA)$_3$^{i}PrPyBox that could limit charge trapping at the Eu sites and cause an unbalanced flow of the charges within the layers is an additional reliable explanation for the limited luminance of Eu(TTA)$_3$^{i}PrPyBox-based devices. The difference in both EQE and maximum luminance (Figure 4A,B) between Eu(TTA)$_3$^{i}PrPyBox-based OLEDs and unpolarized devices (Table 1) in Type-B configuration is larger, and leave room for improvements in designing of more efficient chiral devices architectures.

5 | CONCLUSION

In conclusion, by switching from Phen ancillary ligand to a chiral ^{i}PrPyBox ligand, it is possible to obtain a close relative of the well-known Eu(TTA)$_3$Phen complex, endowed with both a strong CP emission and strong luminescence. The chiral ligand affects the photophysical properties of the Eu(TTA)$_3$^{i}PrPyBox complex in solution and films. The more noticeable difference from optical/photophysical point of view are a slightly lower PLQY and faster decays with respect to Eu(TTA)$_3$Phen. This behavior can be related to both a lower sensitization of the Eu ion and the introduction of additional quenching pathways when the chiral ligand is present.

Further, we obtained CP-OLED devices showing both remarkable emission efficiency (EQE = 1.02% that is comparable to Eu(TTA)$_3$Phen-based OLEDs) and polarization performances ($|g_{EL}| = 0.63$). This was achieved by taking advantage of a modular strategy for the design of the Ln(III) emitter and a selection of proper host matrix for the dispersion of the chiral complex.

This information provides a route to enhance the emission properties of Ln, not limited to visible spectrum, and can be used for application-oriented design of efficient chiral emitters that are compatible with CP-OLED manufacturing process.

ACKNOWLEDGMENTS

Financial support from Italian University and Research Ministry (PRIN Project 20172M3K5N) is gratefully acknowledged. FZ and LDB thank the University of Pisa for financial support (PRA 2020_21 and 2019_23).

DATA AVAILABILITY STATEMENT

The data that support the findings of this study are available from the corresponding authors, [UG or LDB], upon reasonable request.

ORCID

Francesco Zinna https://orcid.org/0000-0002-6331-6219
Lorenzo Di Bari https://orcid.org/0000-0003-2347-2150
Umberto Giovanella https://orcid.org/0000-0003-2865-050X

REFERENCES

1. Zinna F, Giovanella U, Di Bari L. Highly circularly polarized electroluminescence from a chiral europium complex. *Adv Mater*. 2015;27(10):1791-1795. doi:10.1002/adma.201404891
2. Arrico L, Di Bari L, Zinna F. Quantifying the overall efficiency of circularly polarized emitters. *Chem A Eur J*. 2021;27(9):2920-2934. doi:10.1002/chem.202002791
3. Bünzli J-CG, Piguet C. Taking advantage of luminescent lanthanide ions. *Chem Soc Rev*. 2005;34(12):1048-1077. doi:10.1039/b406082m
4. Bünzli J-CG. On the design of highly luminescent lanthanide complexes. *Coord Chem Rev*. 2015;293-294:19-47. doi:10.1016/j.ccr.2014.10.013
5. Wang L, Zhao Z, Wei C, et al. Review on the electroluminescence study of lanthanide complexes. *Adv Opt Mater*. 2019;7(11):1801256. doi:10.1002/adom.201801256
6. Xu H, Sun Q, An Z, Wei Y, Liu X. Electroluminescence from europium(III) complexes. *Coord Chem Rev*. 2015;293-294:228-249. doi:10.1016/j.ccr.2015.02.018
7. Liu Y, Wang Y, He J, et al. High-efficiency red electroluminescence from europium complex containing a neutral dipyrido(3,2-a:2′,3′-c)phenazine ligand in PLEDs. *Org Electron*. 2012;13(6):1038-1043. doi:10.1016/j.orgel.2012.02.024
8. Chen F, Bian Z, Huang C. Progresses in electroluminescence based on europium(III) complexes. *J Rare Earths*. 2009;27(3):345-355. doi:10.1016/S1002-0721(09)00003-9
9. Utochnikova VV, Aslandukov AN, Vashchenko AA, et al. Identifying lifetime as one of the key parameters responsible for the

low brightness of lanthanide-based OLEDs. *Dalton Trans*. 2021;50(37):12806-12813. doi:10.1039/D1DT02269E

10. Kalinowski J, Stampor W, Cocchi M, Virgili D, Fattori V. High-electric-field quantum yield roll-off in efficient europium chelates-based light-emitting diodes. *Appl Phys Lett*. 2005;86(24):241106. doi:10.1063/1.1948512
11. Sano T, Fujita M, Fujii T, Hamada Y, Shibata K, Kuroki K. Novel europium complex for electroluminescent devices with sharp red emission. *Jpn J Appl Phys*. 1995;34(4R):1883. doi:10.1143/JJAP.34.1883
12. Adachi C, Baldo MA, Forrest SR. Electroluminescence mechanisms in organic light emitting devices employing a europium chelate doped in a wide energy gap bipolar conducting host. *J Appl Phys*. 2000;87(11):8049-8055. doi:10.1063/1.373496
13. Male NAH, Salata OV, Christou V. Enhanced electroluminescent efficiency from spin-coated europium(III) organic light-emitting device. *Synth Met*. 2002;126(1):7-10. doi:10.1016/S0379-6779(01)00373-3
14. Bünzli J-CG. Rising stars in science and technology: luminescent lanthanide materials. *Eur J Inorg Chem*. 2017;2017(44):5058-5063. doi:10.1002/ejic.201701201
15. Bünzli J-CG, Eliseeva SV. Intriguing aspects of lanthanide luminescence. *Chem Sci*. 2013;4(5):1939. doi:10.1039/c3sc22126a
16. Shahi PK, Singh AK, Singh SK, Rai SB, Ullrich B. Revelation of the technological versatility of the Eu(TTA)3Phen complex by demonstrating energy harvesting, ultraviolet light detection, temperature sensing, and laser applications. *ACS Appl Mater Interfaces*. 2015;7(33):18231-18239. doi:10.1021/acsami.5b06350
17. Howie JAB, Rowles GK, Hawkins P. An inexpensive sensor for ultraviolet-A and ultraviolet-B radiation. *Meas Sci Technol*. 1991;2(11):1070-1073. doi:10.1088/0957-0233/2/11/012
18. Wang X, Wang T, Tian X, et al. Europium complex doped luminescent solar concentrators with extended absorption range from UV to visible region. *Solar Energy*. 2011;85(9):2179-2184. doi:10.1016/j.solener.2011.06.007
19. Shahi PK, Kumar B, Prakash R, Rai SB. Investigation of optical properties and energy transfer in Eu(III) and Tb(III) based composite compound dispersed in polar, non-polar solvents and polymer matrix. *Mater Res Express*. 2019;6(4):046204. doi:10.1088/2053-1591/aafae8
20. Khalil GE, Lau K, Phelan GD, et al. Europium beta-diketonate temperature sensors: effects of ligands, matrix, and concentration. *Rev Sci Instrum*. 2004;75(1):192-206. doi:10.1063/1.1632997
21. Guimarães LB, Botas AMP, Felinto MCFC, et al. Highly sensitive and precise optical temperature sensors based on new luminescent Tb3+/Eu3+tetrakis complexes with imidazolic counterions. *Mater Adv*. 2020;1(6):1988-1995. doi:10.1039/D0MA00201A
22. Eliseeva SV, Bünzli J-CG. Lanthanide luminescence for functional materials and bio-sciences. *Chem Soc Rev*. 2010;39(1):189-227. doi:10.1039/B905604C
23. Wong H-Y, Lo W-S, Yim K-H, Law G-L. Chirality and Chiroptics of lanthanide molecular and supramolecular assemblies. *Chem*. 2019;5(12):3058-3095. doi:10.1016/j.chempr.2019.08.006
24. Górecki M, Carpita L, Arrico L, Zinna F, Di Bari L. Chiroptical methods in a wide wavelength range for obtaining Ln3+-complexes with circularly polarized luminescence of practical interest. *Dalton Trans*. 2018;47(21):7166-7177. doi:10.1039/C8DT00865E
25. Yuasa J, Ohno T, Miyata K, Tsumatori H, Hasegawa Y, Kawai T. Noncovalent ligand-to-ligand interactions Alter sense of optical chirality in luminescent Tris(β-diketonate) lanthanide(III) complexes containing a chiral Bis(oxazolinyl) pyridine ligand. *J am Chem Soc*. 2011;133(25):9892-9902. doi:10.1021/ja201984u
26. Zinna F, Arrico L, Funaioli T, et al. Modular chiral Eu(iii) complexes for efficient circularly polarized OLEDs. *J Mater Chem C*. 2022;10(2):463-468. doi:10.1039/D1TC05023K
27. Zhang D-W, Li M, Chen C-F. Recent advances in circularly polarized electroluminescence based on organic light-emitting diodes. *Chem Soc Rev*. 2020;49(5):1331-1343. doi:10.1039/C9CS00680J
28. Zinna F, Pasini M, Galeotti F, Botta C, Di Bari L, Giovanella U. Design of Lanthanide-Based OLEDs with remarkable circularly polarized electroluminescence. *Adv Funct Mater*. 2017;27(1):1603719. doi:10.1002/adfm.201603719
29. Freund C, Porzio W, Giovanella U, et al. Thiophene based europium β-Diketonate complexes: effect of the ligand structure on the emission quantum yield. *Inorg Chem*. 2011;50(12):5417-5429. doi:10.1021/ic1021164
30. Moreau J, Giovanella U, Bombenger J-P, et al. Highly emissive nanostructured thin films of organic host-guests for energy conversion. *ChemPhysChem*. 2009;10(4):647-653. doi:10.1002/cphc.200800682
31. Bünzli J-CG, Choppin GR (Eds). *Lanthanide Probes in Life, Chemical and Earth Sciences: Theory and Practice*. Elsevier; 1989.
32. Karimi Behzad S, Amini MM, Ghanbari M, Janghouri M, Anzenbacher P Jr, Ng SW. Synthesis, structure, photoluminescence, and electroluminescence of four europium complexes: fabrication of pure red organic light-emitting diodes from europium complexes. *Eur J Inorg Chem*. 2017;2017(30):3644-3654. doi:10.1002/ejic.201700449
33. Parker D, Fradgley JD, Wong K-L. The design of responsive luminescent lanthanide probes and sensors. *Chem Soc Rev*. 2021;50(14):8193-8213. doi:10.1039/D1CS00310K
34. Fradgley JD, Frawley AT, Pal R, Parker D. Striking solvent dependence of total emission and circularly polarised luminescence in coordinatively saturated chiral europium complexes: solvation significantly perturbs the ligand field. *Phys Chem Chem Phys*. 2021;23(19):11479-11487. doi:10.1039/D1CP01686E
35. Zhang S, Turnbull GA, Samuel IDW. Highly efficient solution-processable europium-complex based organic light-emitting diodes. *Org Electron*. 2012;13(12):3091-3096. doi:10.1016/j.orgel.2012.09.006
36. Okayasu Y, Yuasa J. Evaluation of circularly polarized luminescence in a chiral lanthanide ensemble. *Mol Syst des Eng*. 2018;3(1):66-72. doi:10.1039/C7ME00082K
37. Giovanella U, Betti P, Bolognesi A, et al. Core-type polyfluorene-based copolymers for low-cost light-emitting technologies. *Org Electron*. 2010;11(12):2012-2018. doi:10.1016/j.orgel.2010.09.009
38. Wang Y-F, Li M, Teng J-M, Zhou H-Y, Zhao W-L, Chen C-F. Chiral TADF-active polymers for high-efficiency circularly polarized organic light-emitting diodes. *Angew Chem Int Ed*. 2021;60(44):23619-23624. doi:10.1002/anie.202110794

39. Huang Z, Huang C-W, Tang Y-K, et al. Chiral thermally activated delayed fluorescence emitters for circularly polarized luminescence and efficient deep blue OLEDs. *Dyes Pigments*. 2022;197:109860. doi:10.1016/j.dyepig.2021.109860
40. Greenfield JL, Wade J, Brandt JR, Shi X, Penfold TJ, Fuchter MJ. Pathways to increase the dissymmetry in the interaction of chiral light and chiral molecules. *Chem Sci*. 2021;12(25):8589-8602. doi:10.1039/D1SC02335G
41. Liu N, Mei S, Sun D, et al. Effects of charge transport materials on blue fluorescent organic light-emitting diodes with a host-dopant system. *Micromachines*. 2019;10(5):344. doi:10.3390/mi10050344
42. D'Angelo P, Barra M, Cassinese A, et al. Electrical transport properties characterization of PVK (poly N-vinylcarbazole) for electroluminescent devices applications. *Solid-State Electron*. 2007;51(1):123-129. doi:10.1016/j.sse.2006.11.008
43. Katkova MA, Bochkarev MN. New trends in design of electroluminescent rare earth metallo-complexes for OLEDs. *Dalton Trans*. 2010;39(29):6599-6612. doi:10.1039/c001152e

SUPPORTING INFORMATION

Additional supporting information can be found online in the Supporting Information section at the end of this article.

How to cite this article: Zinna F, Pasini M, Cabras M, et al. Impact of chiral ligands on photophysical and electro-optical properties of β-diketonate europium complexes in circularly polarized OLEDs. *Chirality*. 2023;35(5):270-280. doi:10.1002/chir.23538